International Journal of Power Electronics and Drive System (IJPEDS)
Vol. 10, No. 3, Sep 2019, pp. 1613~1627
ISSN: 2088-8694, DOI: 10.11591/ijpeds.v10.i3.1613-1627

Control of the photoelectric generator for used in feeding of the independent wind turbine system

Mohammed Kendzi[1], Abdelghani Aissaoui[2], Mohamed Abid[3], Ahmed Tahour[3]
[1]Department of Electrical Engineering, Smart Grids and Renewable Energies Laboratory,
Tahri Mohammed Bechar University, Algeria
[2]Department of Electrical Engineering, Tahri Mohammed Bechar University, Algeria
[3]Department of Electrical Engineering, IRECOM Laboratory, Djilali Liabes of Sidi Bel Abbes University, Algeria

Article Info

Article history:

Received Dec 7, 2017
Revised Feb 14, 2019
Accepted Apr 8, 2019

Keywords:

Wind turbine
Doubly fed induction generator
Photovoltaic
Fuzzy logic
Control of power

ABSTRACT

In this paper, a hybrid power system is proposed to eliminate any interruption caused to absence of power supply network by the Fusion between the wind source and the photovoltaic source to create a hybrid system with internal power supply autonomy. The hybrid power system includes a solar and wind source whose wind energy conversion system is based on a doubly fed induction generator. The photovoltaic conversion system extracts the maximum power from the sun. A part of this power is used to supply the rotor of a doubly fed induction generator; the rest is injected in the grid. The connection between the two conversion systems is made by means of static converters (chopper/inverter). In the photovoltaic conversion chain, a controller for tracking the maximum power point is designed using the direct search approach the Perturb and observe method. The wind energy conversion system contains a doubly fed asynchronous generator with a control system of generated powers by the technique of the fuzzy logic. The simulation was done to prove the validity of the strategy and of the control method used for the control of the power generated by the hybrid system.

Corresponding Author:

Mohammed Kendzi,
Department of Electrical Engineering,
Smart Grids and Renewable Energies Laboratory,
Tahri Mohammed Bechar University,
University of Tahri Mohamed,
Bechar, B.P 417 Bechar 08000, Algeria.
Email: kendzimohammed@gmail.com

1. INTRODUCTION

Renewable energies have become very promising sources of future energy resources in the world, primarily because of their own nature, and also because of the diminishing reserves of traditional resources (oil, gas, etc.). .), Demographic and economic growth [1, 2]. Where the use of these sources to generate electricity has been seen since the last decade [3]. The main advantage of renewable sources is the absence of harmful emissions. One way to generate electricity from renewable sources is to use wind and photovoltaic power, mainly because it is clean [4]. The hybrid system is achieved in renewable energies consisting of wind energy and photovoltaic (PV) energy for parallel performance of these two sources, ensuring DFIG training and maximizing power generation with better efficiency [5, 6] through the integration of foggy logic technology to ensure control of powers Deposited towards the network.

This control technology is simple in its implementation and its relatively satisfactory efficiency (for some applications), and the ease of operation and low cost of these controllers are the main reasons for its success [7]. Fuzzy logic is therefore one of the important branches of artificial intelligence among all intelligent techniques, the simplest method of control to be implemented in practice. [8, 9].

The work presented in this paper relates to the implementation of the DFIG wind turbine control strategy and the supply of rotor from a PV generator. This system is controlled by foggy logic technology. The regulation of this paper is as follows: In Section 2, we introduce the proposed mixed system (PV/wind). 3rdsection was designed to model hybrid system components. In Section 4, a control strategy is presented. In Section 5, the principle of precise logical control is described and used in the design of misty logical controllers. The photovoltaic system model is achieved in Section VI. In Section 7, we describe the MPPT structure applied to the PV system. The simulation results and conclusions are summarized in the last sections

2. PRESENTATION OF THE HYBRID SYSTEM (PHOTOVOLTAIC/WIND)

The hybrid power system contains two conversion chains. The first chain is a wind power conversion system, containing a DFIG connected directly to the networks. The second chain is a photovoltaic conversion system. The power generated by the DFIG is controlled by the technique of the fuzzy logic. The PV generator is used to supply the DFIG rotor, while the rest of the generated power is injected into the grid. Figure 1 shows the block diagram of the proposed hybrid power system.

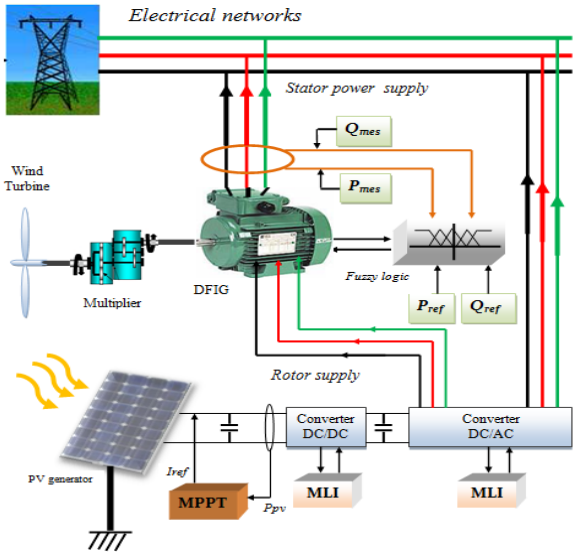

Figure 1. Block diagram the hybrid power system

3. MODELING OF TNE CONVERSION HYBRID SYSTEM

3.1. Model of the turbine

The aeroturbine is composed of three pales of length R on one tree, a turbine and a gearbox with a gain G. The generator shaft is modeled by the following equation [10]:

$$J\frac{d}{dt}\Omega_{mec} = C_g - C_{em} - f\Omega_{mec} \quad (1)$$

$$C_g = \frac{C_{aer}}{G}, C_{aer} = \frac{P_{aer}}{\Omega_{tur}}, \Omega_{mec} = G\Omega_{tur} \quad (2)$$

Where: J is the total inertia of rotating parts (kg • m^2); f is the viscous friction coefficient; C_{em} is the electromagnetic torque of the generator (N • m); C_g is the mechanical torque in the output of the multiplier; C_{aer} is the aerodynamic torque of the turbine; G is the multiplier gain; Ω_{mec} is generator speed; Ω_{tur} is the speed of the turbine. In the wind turbine model, the aerodynamic power output is given as follows:

$$P_{aer} = C_p(\lambda;\beta)\frac{\rho}{2} s v^3 \quad (3)$$

Where ρ is the air density (Kg/m^3), v is the wind speed (m/s), and C_p is the power coefficient.

The power coefficient C_p presents the portion of wind power captured by the turbine. It depends on two parameters, namely tip speed ratio λ and pitch angle of the blades β: [11, 12]:

$$C_p = 0.5 - 0.00167(\beta - 2)\sin\left[\frac{\pi(\lambda + 0.1)}{18.5 - 0.3(\beta - 2)}\right] - 0.00184(\lambda - 3)(\beta - 2) \quad (4)$$

Where: λ is the speed ratio is defined as the ratio between the linear speed of the blades and the wind speed; β is the orientation angle of the blades.

3.2. Modeling of DFIG

The Park model of the machine is described by the following equations [13, 14]: The electric equations:

$$\begin{cases} v_{ds} = R_s i_{ds} + \frac{d}{dt}\phi_{ds} - \omega_s \phi_{qs} \\ v_{qs} = R_s i_{qs} + \frac{d}{dt}\phi_{qs} - \omega_s \phi_{ds} \\ v_{dr} = R_r i_{dr} + \frac{d}{dt}\phi_{dr} - (\omega_s - \omega_r)\phi_{qr} \\ v_{qr} = R_r i_{qr} + \frac{d}{dt}\phi_{qr} + (\omega_s - \omega_r)\phi_{dr} \end{cases} \quad (5)$$

The flux equations:

$$\begin{cases} \phi_{ds} = L_s i_{ds} + M_{sr} i_{dr} \\ \phi_{qs} = L_s i_{qs} + M_{sr} i_{qr} \\ \phi_{dr} = L_r i_{dr} + M_{sr} i_{ds} \\ \phi_{qr} = L_r i_{qr} + M_{sr} i_{qs} \end{cases} \quad (6)$$

The electromagnetic torque equation:

$$C_{em} = p\frac{M_{sr}}{L_s}\left(\phi_{qs} i_{dr} - \phi_{ds} i_{qr}\right) \quad (7)$$

where: R_s is the stator resistance, R_r is the rotor resistance, L_s is the stator inductance, M_{sr} is mutual inductance, ϕ_{ds}, ϕ_{qs} are respectively the direct and quadrature fluxes of the stator, ϕ_{dr}, ϕ_{qr} are respectively the direct and quadrature fluxes of the rotor, i_{ds}, i_{qs} are respectively direct and quadrature stator currents, i_{dr}, i_{qr} are respectively direct and quadrature rotor currents, p is number of even poles, ω_r, ω_s are angular speeds respectively of the rotor and stator.

4. CONTROL STRATEGY

The active and reactive powers are written in the Park model as follows [15, 16]:

$$\begin{cases} P_s = V_{ds} i_{ds} + V_{qs} i_{qs} \\ Q_s = V_{qs} i_{ds} - V_{ds} i_{qs} \end{cases} \quad (8)$$

By the orientation of the stator flux along the axis *d,* we have:

$$\phi_{qs} = 0 \quad , \quad \phi_{ds} = \phi_s \tag{9}$$

and

$$V_{qs} = V_s \ , \ V_{ds} = 0 \tag{10}$$

The (8) becomes:

$$\begin{cases} P_s = V_{qs} i_{qs} \\ Q_s = V_{qs} i_{ds} \end{cases} \tag{11}$$

By combining (5, 6, and 11), (11) becomes:

$$\begin{cases} P_s = -V_s \dfrac{M}{L_s} i_{qr} \\ Q_s = -V_s \dfrac{M}{L_s} i_{dr} + \dfrac{V_s \phi_s}{L_s} \end{cases} \tag{12}$$

By substituting (6) for (5) and using (9), the rotor voltage can be rewritten as follows:

$$\begin{cases} v_{dr} = R_r i_{dr} + \sigma L_r \dfrac{di_{dr}}{dt} - g \omega_s \sigma L_r i_{qr} \\ v_{qr} = R_r i_{qr} + \sigma L_r \dfrac{di_{qr}}{dt} + g \omega_s \sigma L_r i_{dr} + g \dfrac{M V_s}{L_s} \end{cases} \tag{13}$$

Where : $\sigma = 1 - \dfrac{M^2}{L_r L_s}$; $g = 1 - \dfrac{\omega_s}{\omega_r}$

5. FUZZY LOGIC CONTROL

5.1. Principle of fuzzy logic method

The principle of fuzzy control is based on the following three blocks: Fuzzification of input variables which are defined by linguistic variables (fuzzy sets or subsets), then the Inference where these variables are compared with predefined sets to determine appropriate response. And finally defuzzification, to convert the subset fuzzification in values, using the centroid defuzzification. The basic structure of our fuzzy controller is shown in Figure 2 [17, 18].

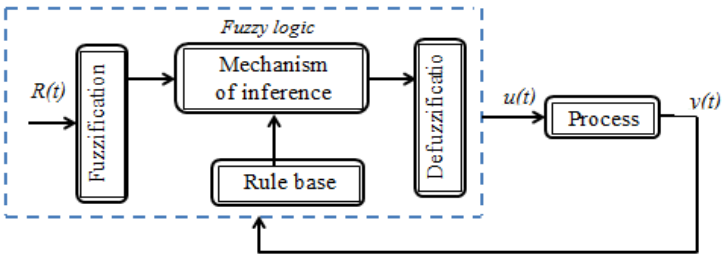

Figure 2. Internal structure of a fuzzy controller

With: R(t) is the reference signal, u(t) is the command signal, y(t) is the output of the system to be controlled.

5.2. Regulating power by fuzzy logic

The fuzzy controller is basically non-linear static input/output plot as show in Figure 3, the controller action can be written in the form:

$$u = k_e.e + k_{\Delta e}.\Delta e \tag{14}$$

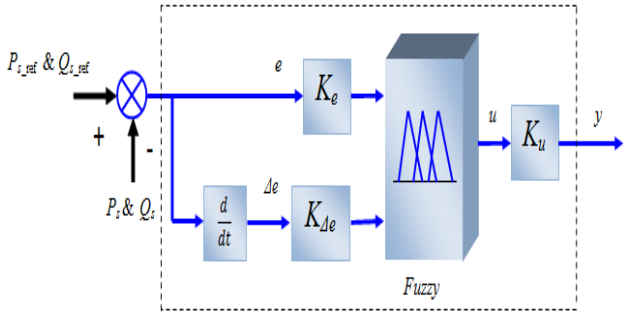

Figure 3. Fuzzy logic regulator

The fuzzy output is:

$$y = k_u.u \tag{15}$$

Where: k_e is the gain of the power error (P_s or Q_s), $k_{\Delta e}$ is the gain of the variation of the power error (P_s *or* Q_s); e is the power error (P_s or Q_s), Δe is the variation of the error of (P_s or Q_s), u is the fuzzy output.
The error, e is defined by:

$$\begin{cases} e(k) = P_S(k) - P_{S\_ref}(k) \\ e(k) = Q_S(k) - Q_{S\_ref}(k) \end{cases} \tag{16}$$

Where: $P_{s\ ref}$ is the reference stator power active, Q_{s_ref} is the reference reactive stator power, Δe is the variation of the error, it is approximated by:

$$\Delta e(k) = e(k) - e(k-1) \tag{17}$$

5.3. Structure and application of a fuzzy adjustment of the stator power in a DFIG

In this section, we supposed the fuzzy controller with five fuzzy subsets and constructed from the following condition rule:

Rule (i) : if s is F^i_s , then u_f is F^i_{uf} , i=1,…,5

Table 1 shows one of possible control rules based on five membership functions, where: *NB* is negative big, *NS* is negative small, *ZE* is zero, *PS* is positive small and *PB* is positive big. These acronyms are labels of fuzzy sets and their corresponding membership functions are depicted in Figure 4, [19]. To control the stator power in a DFIG we have using the block diagram of Figure 5 similar to that of Figure 3.

Table 1.one of possible control rules based on five membership functions

e	Δe				
	NB	*NS*	*ZE*	*PS*	*PB*
NB	*ZE*	*ZE*	*PB*	*PB*	*PB*
NS	*ZE*	*ZE*	*PS*	*PS*	*PS*
ZE	*PS*	*ZE*	*ZE*	*ZE*	*NS*
PS	*NS*	*NS*	*NS*	*ZE*	*ZE*
PB	*NB*	*NB*	*NB*	*ZE*	*ZE*

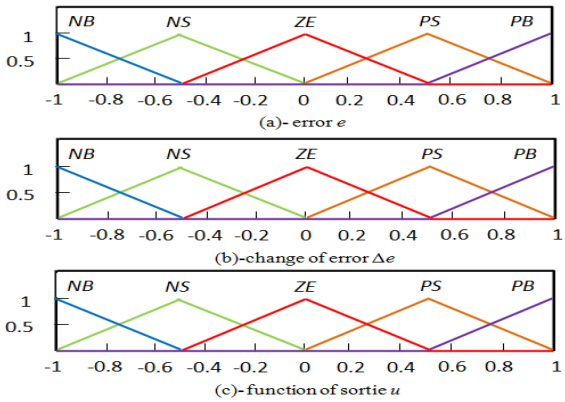

Figure 4. Membership functions of: (a) error e; (b) change of error Δe; (c) function of sortie u

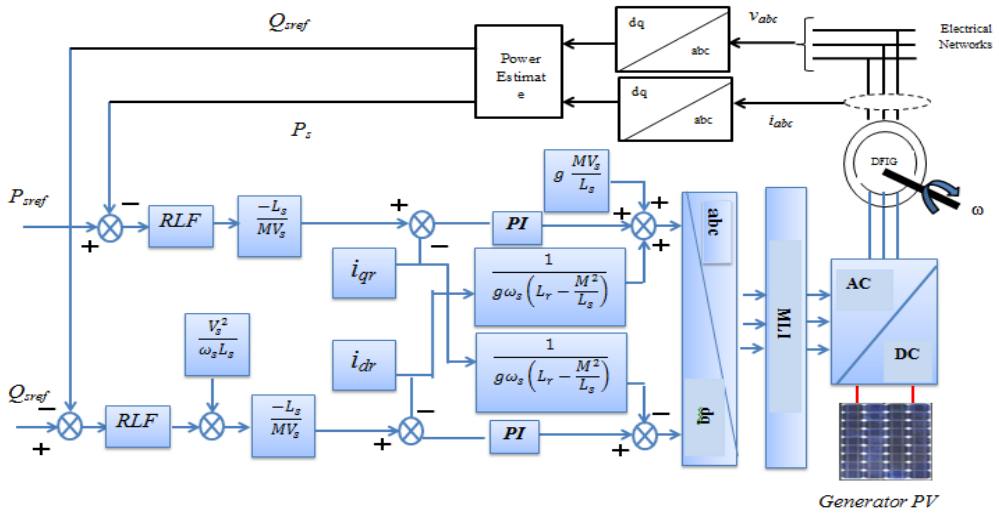

Figure 5. Structure of a fuzzy adjustment of the stator power of a DFIG generator

6. MODELING OF THE PHOTOVOLTAIC ENERGY CONVERSION SYSTEM

This system consists of a PV solar generator directly connected with the chopper coverter through a bus continuous to feed the inverter converter with the DC voltage, which in turn feeds the rotor DFIG with the alternative voltage. A PV module consists of a number of solar cells connected in series and parallel to obtain the desired voltage and current output levels. As sunlight strikes a solar cell, the incident energy is converted directly into electrical energy. Single-diode mathematic model is applicable to simulate silicon photovoltaic cells, which consists of a photocurrent source, a nonlinear diode, and internal resistances, as shown in Figure 6.

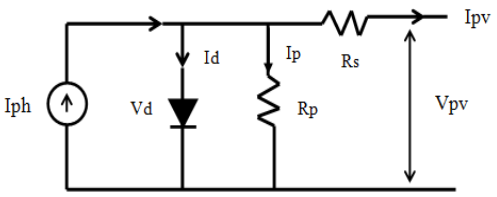

Figure 6. Equivalent diagram of a real photovoltaic cell [20]

$$I_{pv} = I_{ph} - I_d - I_p \tag{18}$$

$$I_{pv} = I_{ph} - I_d = I_{ph} - I_0\left(\exp\left(\frac{e\left(V_{pv} + I_{pv}R_s\right)}{mKT_c}\right) - 1\right) - \frac{V_{pv} + I_{pv}R_s}{R_p} \tag{19}$$

$$I_0 = 1.5 \times 10^5 \exp\left(\frac{-E_g}{KT_c}\right) \tag{20}$$

Where: I_o is the saturation current of the unlit junction; I_c is the current of the cell; e is the charge of the electron (1.6 x10^{-19}C); K is Boltzmann's constant (1.38 x10^{-23}J / K); T_c is the junction temperature of the photovoltaic cell; m is the ideality factor of the junction; V_{pv} is the voltage across the cell; R_s is the series resistance; R_p is the shunt resistor. E_g is the energy of the forbidden band for a semiconductor material gives, E_g is almost constant and I_0 is therefore a function of the temperature.

6.1. Modeling of the photovoltaic continuous bus

The evolution of the photovoltaic DC bus voltage is given by the following equation:

$$v_{pv} = \frac{1}{c_{pv}} \int i_{c_{pv}} dt \tag{21}$$

The current in the photovoltaic DC bus comes from a node from which two currents flow:

$$i_{c_{pv}} = i_{pv} - i_{hac} \tag{22}$$

Where: I_{cpv} is the current of the photovoltaic continuous bus; I_{hac} is the current of the chopper; C_{pv} is the capacity of the photovoltaic continuous bus.

6.2. Chopper booster

The booster converter controls the electrical power in DC circuits with great flexibility and high efficiency. It consists of capacitors, inductance, and switches; all these devices consume no active power.

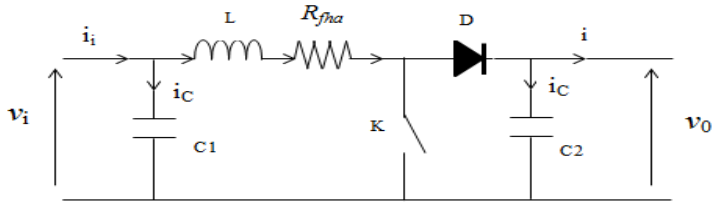

Figure 7. Electrical Boost converter Scheme [21]

During operation of the chopper, the transistor switches at a constant frequency fs with a closing time (αTs) and an opening time ((1-α) T_s.) where:
- Ts is the switching period that equals (1/f_s)
- α : the cyclic ratio of the switch ($\alpha \in [0, 1]$).

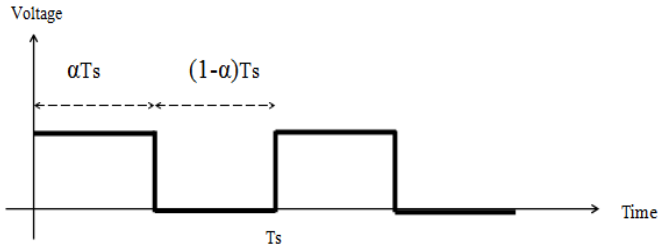

Figure 8. Periods of closing and opening a switch.

Applying Kirchhoff's laws to the scheme of figure 7, we obtain the following systems of equations [22]:
For the 1st period $\alpha.T_s$:

$$\begin{cases} i_{c_1}(t) = c_1 \dfrac{dv_i(t)}{dt} = i_i(t) - i_L(t) \\ i_{c_2}(t) = c_2 \dfrac{dv_0(t)}{dt} = -i_0(t) \\ v_L(t) = L \dfrac{di_L}{dt} = -v_i(t) - R_L i_L \end{cases} \tag{23}$$

For the 2nd period $(1-\alpha).T_s$:

$$\begin{cases} i_{c_1}(t) = c_1 \dfrac{dv_i(t)}{dt} = i_i(t) - i_L(t) \\ i_{c_2}(t) = c_2 \dfrac{dv_0(t)}{dt} = i_L(t) - i_0(t) \\ v_L(t) = L \dfrac{di_L}{dt} = v_i(t) - v_0(t) - R_L i_L \end{cases} \tag{24}$$

To find a valid dynamic representation for the whole period T_s, we generally use the following expression:

$$\frac{dx}{dt} T_s = \frac{dx}{dt_{(\alpha T_s)}} \alpha T_s + \frac{dx}{dt_{((1-\alpha)T_s)}} (1-\alpha) T_s \tag{25}$$

Applying the relation (25) to the systems of equations (23) and (24), we find the Equations that govern the system over an entire period are obtained:

$$\begin{cases} c_1 \dfrac{dv_i}{dt} T_s = \alpha T_s (i_i - i_L) + (1-\alpha) T_s (i_i - i_L) \\ c_2 \dfrac{dv_0}{dt} T_s = -\alpha T_s i_0 + (1-\alpha) T_s (i_L - i_0) \\ L \dfrac{di_L}{dt} T_s = \alpha T_s (v_i - R_L i_L) + (1-\alpha) T_s (v_i - v_0 - R_L i_L) \end{cases} \tag{26}$$

By arranging the terms of the preceding equations, (so that we can interconnect the Boost with the other simulation blocks), we obtain the dynamic modeling of the Boost converter:

$$\begin{cases} i_L = i_i - c_1 \dfrac{dv_i(t)}{dt} \\ i_0 = (1-\alpha) i_L - c_2 \dfrac{dv_0(t)}{dt} \\ v_i = L \dfrac{di_L}{dt} + (1-\alpha) v_0 + R_L i_L \end{cases} \tag{27}$$

6.3. Modeling the chopper filter

A filter is used to eliminate the harmonics generated by the chopper. The evolution of the filter voltage is given by the following equation [13]:

$$v_{fhac} = R_{fhac} i_{fhac} + L_{fhac} \frac{di_{fhac}}{dt} \quad (28)$$

Where: R_{fhac} is the chopper filter resistance; L_{fhac} is chopper filter inductance.

6.4. Chopper control

Adjusting of the voltage according to the desired power (reference) is necessary to control the energy produced by the GPV photovoltaic generator with a modification of the variable control of the chopper (periodic ratio α) and servocontrol of the ifhac filter current (ifhac). In our study, the switch of the converter is controlled by a Pulse wave Modulation Large (PWM) signal, with a fixed frequency fs and a cyclic ratio α variable. The two operating phases of the switch *S* must be studied to extract the control law of the photovoltaic generator power output [23]:

- S_{hac} is closed ($0<t<\alpha T_s$):

$$\frac{di_{fhac}}{dt} = \frac{1}{L_{fhac}}\left(v_{pv} - v_{dc} - R_{fhac} i_{fhac}\right) \quad (29)$$

- S_{hac} *is open* ($\alpha Ts<t<Ts$):

$$\frac{di_{fhac}}{dt} = -\frac{1}{L_{fhac}}\left(v_{dc} + R_{fhac} i_{fhac}\right) \quad (30)$$

Term (29) and (30) represent the equations of the chopper and its filter for a period αTs and $(1-\alpha)Ts$ respectively. So we have to find a valid approximated dynamic representation for both time slots. For this and from equation (25) we consider that the variation of the dynamic variable (i_{fhac}) is of linear form, so the derivative of the dynamic variable (i_{fhac}) can be defined according to equation (25) over the two time periods αTs and $(1-\alpha)Ts$:

$$\frac{di_{fhac}}{dt} T_s = \frac{di_{fhac}}{dt_{(\alpha T_s)}} \alpha T_s + \frac{di_{fhac}}{dt_{\left((1-\alpha)T_s\right)}} (1-\alpha) T_s \quad (31)$$

By replacing (29) and (30) by their value in relation (31) we obtain the equation that governs the system on the entire period:

$$\frac{di_{fhac}}{dt} = \frac{1}{L_{fhac}}\left(\alpha v_{pv} - v_{dc} - R_{fhac} i_{fhac}\right) \quad (32)$$

The control law is given by the following expression and descripted in Figure 9:

$$\alpha = \frac{v_{fhac} + v_{dc}}{v_{pv}} \quad (33)$$

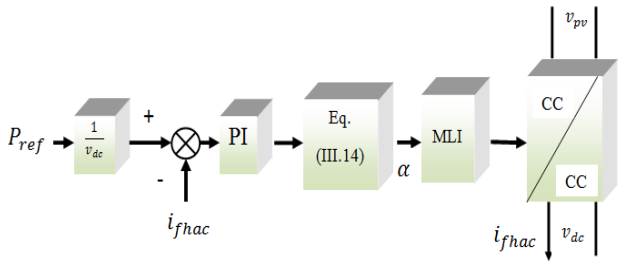

Figure 9. Chopper control.

7. STRUCTURE OF THE MPPT COMMAND BY THE METHOD OF DISTURBANCE AND OBSERVATION « P & O »

The "P & O" disturbance and observation method is a widely used approach in the search for Maximum Power Point Tracking (MPPT) because it is simple and requires only voltage and current measurements of the photovoltaic panels vpv and ipv respectively. It can be used to deduce the point of maximum power even during variations in illumination and temperature.

7.1 Reference current calculation by program of the MPPT command

Several algorithms have been proposed for the realization of the MPPT command for that we have chosen the following program:

```
% Simple MPP "perturb and observe" tracking algorithm
% using Boost DC-DC input current Iref as the control variable
% Pold, Iref and Increment are initialized in Initialize MPPtrackIref.m
% Input: power P to be maximized
% Output: reference current
function y = fcn(Ppv)
global Pold;
global Iref;
global Increment;
IrefH = 5; % upper limit for the reference current
IrefL = 0; % lower limit for the reference current
DeltaI = 0.02; % reference current increment
P = Ppv
if (P < Pold)
Increment = -Increment; % change direction if P decreased
end
% increment current reference
Iref=Iref+Increment*DeltaI;
% check for upper limit
if (Iref > IrefH)
 Iref = IrefH;
End
% check for lower limit
if (Iref < IrefL)
Iref = IrefL;
End
% save power value
Pold = P;
% output current reference
y = Iref;
```

8. SIMULATIONS AND RESULTS

Simulation of the proposed system has been realized using Matlab/Simulink. The parameters of Simulation are given in appendix. The DFIG is connected directly through its stator to the network and his rotor to the cycloconverter (the inverter DC/AC) of the photovoltaic energy conversion system as show in Figure 10. The first part of simulation consists of the regulation system of the DC voltage obtained by the chopper.

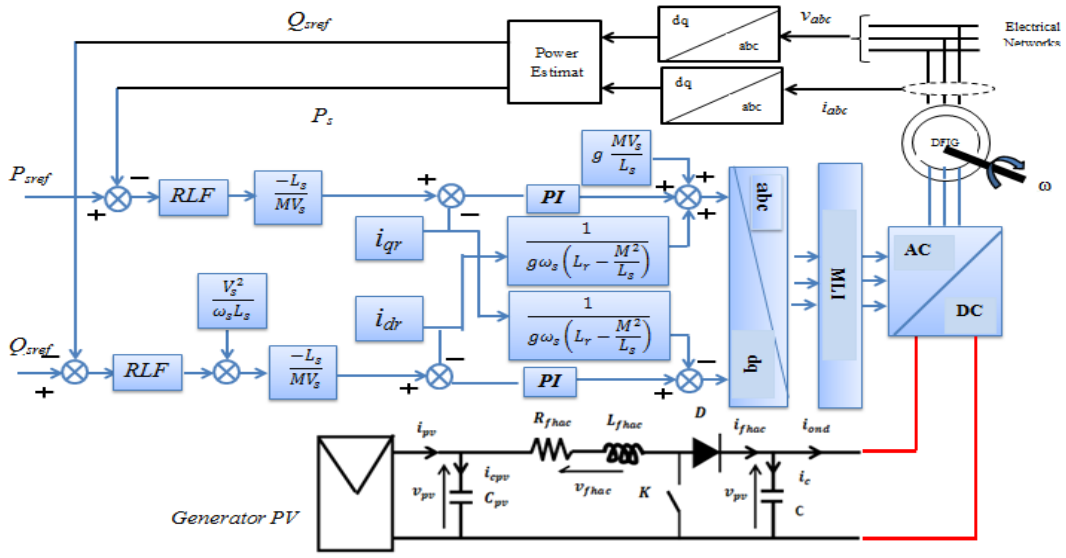

Figure 10. Control of the stator powers of the hybrid system by fuzzy logic

In this section, the system described in Figure 10 was simulated in Matlab-Simulink. The first part of the simulation focuses on the regulation system of the DC voltage obtained by the chopper (regular at 330V) which feeds the inverter and then the rotor of the DFIG in along field changes of solar radiation. To achieve the control of the stator powers generated by the DFIG, the fuzzy logic controller is used as described in Figure 3. The second part focuses on the control system of the photovoltaic generator as described in Figure 6, where the goal is to extract the maximum power of solar sources. A part of this power is used to supply the rotor of the DFIG. The rest is injected into the grid. Finally we have a comparison between two systems, one is a classical system (rotor supply via electrical networks) and the other is a system that contains our proposal (rotor supply via a photovoltaic panel).

The voltage of the chopper v_{dc} is maintained at 330V as shown in Figure 11. A transition period be distinguished in the interval t = [0 0.04] s. After this period, the chopper voltage is maintained constant along the field changes of solar radiation as show in Figure 12.

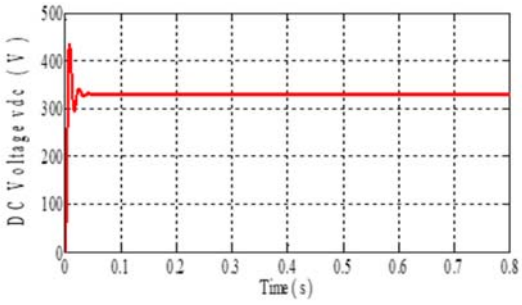

Figure 11. The obtained chopper voltage v_{dc}

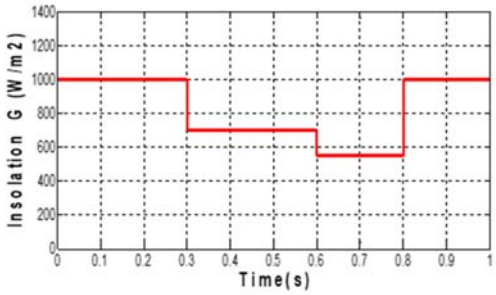

Figure 12. Vareation of solar radiation G

In Figure 13, we have changes in the sequential reference current for solar radiation changes (Figure 11). This current is used in the MPPT command program to track the maximum power point. The control of the active and reactive powers (P_s , Q_s) delivered by the generator DFIG is ensured by the fuzzy logic regulator. After simulating the system by means of Simulink / MATLAB, a fast acceptable variation of the voltage v_{rabc} and the current I_{rabc} which supplies the rotor of the DFIG shown in Figures 14 and 15 has been found.

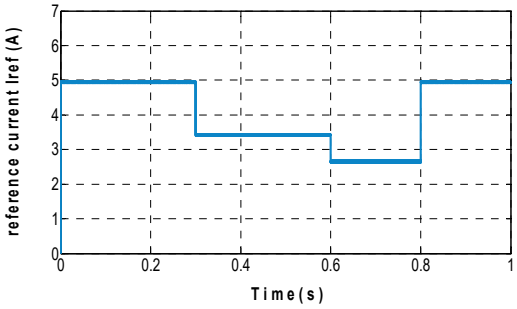

Figure 13. Vareation of reference current of MPPT I_{ref}

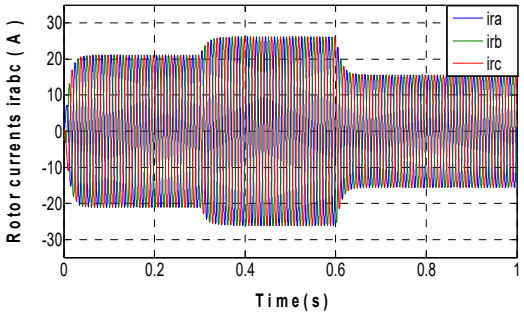

Figure14. Rotor currents

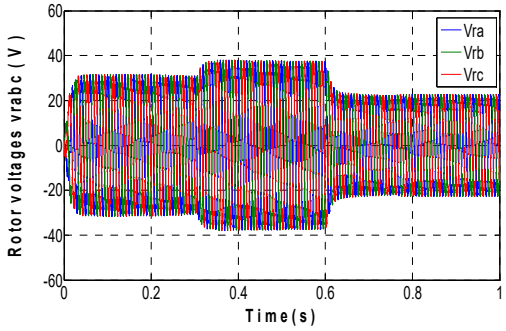

Figure 15. Rotor voltages

Figure 16 and 17 show the regulation of active and active fixed power as a function of time at different times. At time t = 0.3s, the active and reactive power were adapted to the values of 4kW and 1kvar, respectively. A: t = [0.3 0.6] s: the active power was adapted to the value 5 kW, the reactive power to the value 2kvar. At time t = 0.6s they decreased to the values of P_s = 3 kW and Q_s = 1.5kvar.

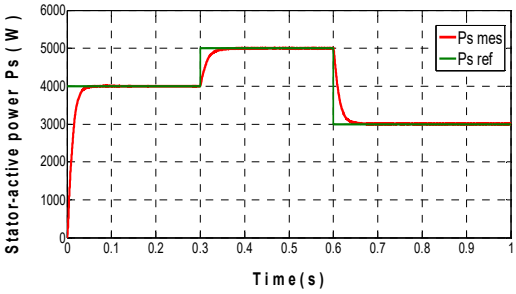

Figure 16. Stator-active power after control and regulation

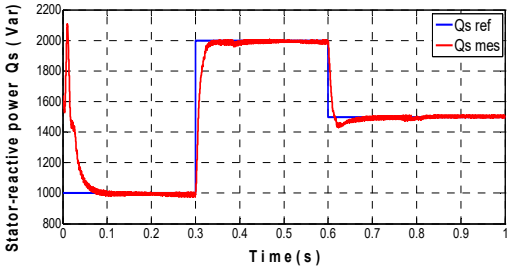

Figure 17. Stator-reactive power after control and regulation

For the energy produced by the photovoltaic generator show in Figure 18, it changes according to the vareation of solar radiation refer Figure 11 and reference current refer Figure 13. In parallel to the production of power output at the stator, we have consumption of internal energy by the rotor generator, this energy changes over time with change in energy levels required at the level of stator as show in Figure 19. At time t = 0.3s, the rotor power of DFIG consumed 317W. A: t = [0.3 0.6] s: this consumption up to 477W, and he down to 182W at time t = 0.6s. We can be used the residual energy produced by the photovoltaic generator after subtracting energy consumed from the rotor to charge the batteries and can be injected in to the grid as shown in Figure 20.

In this section we have varation of the active and reactive powers stator P_{sa}, Q_{sa} and P_s, Q_s of the two sytem, one is a classical system (rotor supply via electrical networks) and the other is a system that contains our proposal (rotor supply via a photovoltaic panel), respectively as show in Figure 21. A: t = [0 0.25] s, we have tow systems work in the normal state. A: t = [0.25 0.4] s and t= [0.6 0.78] s, we have Lack in power of the electricity grid which causes a lack of production at the level of the classical system (P_s=4kw, Q_s= 1kvar and P_{sa}=0kW, Q_{sa}= 0kvar). So the classical system is affected by network interruptions and our system proposed is remains stable.

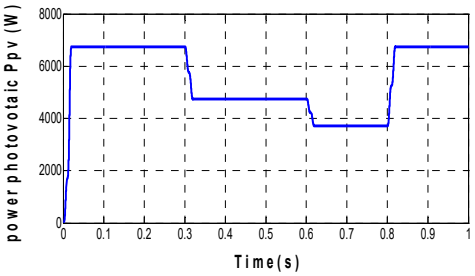

Figure 18. PV generated power

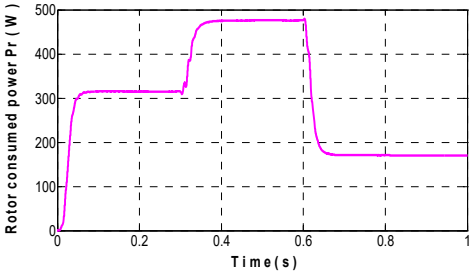

Figure 19. Rotor consumed power

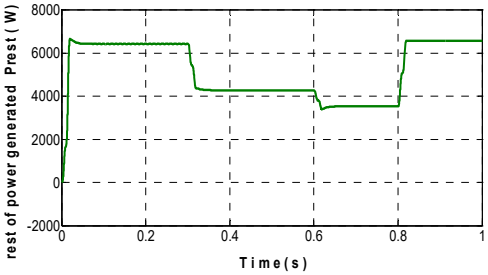

Figure 20. The rest of the power generated by the PV

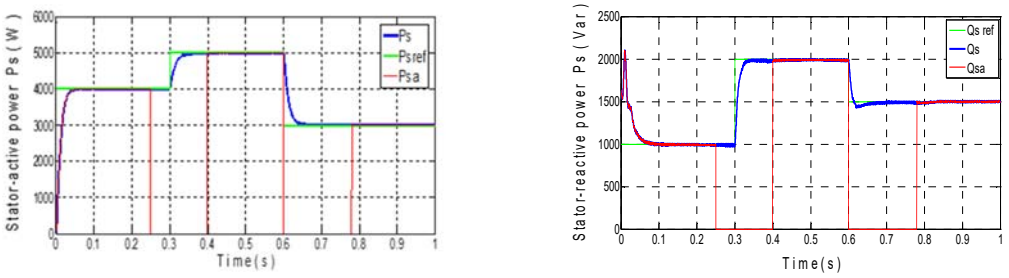

Figure 21. Variation of active and reactive Stator power and reaction of tow systems deffirent after interruption of network power

9. CONCLUSION

In this paper, a hybrid energy conversion system combining photovoltaic and wind turbines as a scale alternative source of electrical energy is proposed. The power is generated by means of photovoltaic and wind energy while maintaining the energy efficiency and the reliability of the system. A complete description of the hybrid system was presented along with the detailed simulation results that prove its usefulness and In this context, maximum power was extracted under the operating conditions of the PV generator, and part of this energy was used to supply the DFIG rotor used in wind system and inject the rest of the energy into the grid. To adjust the power produced in the stator of DFIG was used the technique of the fuzzy logic because he is the simplest control technique Applied in practice. To extracted maximum power in photovoltaic systeme, we have used the tracking technique of maximum power point because she is simple and cost-effective. At the end, the entire circuit simulation was developed in a MATLAB/SIMULINK environment and the result based on the various simulations of the performance of system in different situations was presented and efficiency of the system proposed with classical system.

APPENDIX

Parameters of the system simulation
Photovoltaic generator
Insolation: G : [550 1000] W/m^2
Short circuit current: I_{sc} : 5.45A
Open circuit voltage: V_{oc} : 22.2V
Current at Pmax : I_r : 4.95A
Voltage at Pmax : V_r : 17.2V
Cell number in series : 2
Cell number in Parallel : 44

Wind generator
Power: P: 7.5 KW
Stator voltage: V_s: 220V
Rotor resistance: R_r: 1.8Ω
Stator resistance: R_s : 0.95Ω
Rotor inductance: L_r : 0.088H
Stator inductance: L_s : 0.094H
Mutual inductance: M : 0.082H

REFERENCES

[1] M.Z.F.Z. Zerhoun, "Optimization of a green energy system with practical validation," *Revue des énergies renouvelables*, vol. 11, n°1, pp. 41-49, 2008.
[2] F. Tati and O. Ben Lamoudi, "Study and Realization of an Optimized Photovoltaic System by Fuzzy Logic," *Phd thesis in Electrical Engineering, universite kasdi merbah ouargla*, 2018.
[3] V. C. Ganti, B. *et al.*, "DFIG based Wind power conversion with grid power leveling for reduced gusts," *IEEE Trans. On Sustainable energy*, vol.3, n°.1, pp. 12-19, January 2012.
[4] P. A. Tapia, *et al.*, "Modeling and control of a wind turbine driven doubly fed induction generator," *IEEE Trans. On Energy conversion*, vol. 18, no. 2, June 2003
[5] S. Arezki and M. Boudour, "study and regulation of DC bus voltages of wind-photovoltaic system," *Rev. Roum. Sci. Techn. – Électrotechn. et Énerg*, 59, 1, p. 35–46, Bucarest, 2014
[6] S. El Aimani, "Modeling of Different Integrated Wind Turbine Technologies in a Medium Voltage Network", *Phd thesis in Electrical Engineering, University of Science and Technology of Lille*, France, 2004.
[7] B. Ferdi, *et al.*, "Statcom DC-bus Voltage Fuzzy Controller Design using ANFIS," *Acta Electrotrhnica*, vol. 55, pp. 32 – 38, 2014.
[8] P. Ponce, *et al.*, "Doubly Fed Induction Generator (DFIG) Wind Turbine Controlled by Artificial Organic Networks, " *Soft Computing, Methodologies and Application, Springer*, vol. 22, pp. 2867–2879, 2018.
[9] A. Tamaarat and A. Benakcha, "Performance of Active and Reactive Power Control in a DFIG -based Wind Turbine, " *Revue des Energies Renouvelables,* vol. 20, n°4,pp. 635 – 647, 2017.
[10] M. Adjoudj, *et al.*, "Sliding Mode Control of a Doubly Fed Induction Generator for Wind Turbines," *Rev. Roum. Sci. Techn. – Electrotechn. Energ*, vol. 56,1, pp. 15-24, 2011
[11] O. Zamzoum, *et al.*, "Power control of variable speed wind turbine based on doubly fed induction generator using indirect field- oriented control with fuzzy logic controllers for performance optimization," *Energy Sci Eng.* vol. 6, pp. 408-423, 2018.

[12] Md. Rifat Hazari, *et al.*, "Stability Augmentation of a Grid-Connected Wind Farm by Fuzzy-Logic-Controlled DFIG-Based Wind Turbines," *Appl. Sci*, 8, 20, pp. 1-24, 2018, doi: 10.3390/app8010020,
[13] A. Boumassata and D. Kerdoun, "Modeling, Simulation and Control of Wind Energy Conversion System based on Doubly Fed Induction Generator and Cycloconverter," *Advances in Electrical and Computer Engineering*, vol.14, n°2,pp. 43-48, 2014
[14] K. Belgacem, *et al.*, "Design and Analysis of Adaptive Sliding Mode with Exponential Reaching Law Control for Double-Fed Induction Generator Based Wind Turbine," *International Journal of Power Electronics and Drive System (IJPEDS)*, vol. 9, no. 4, pp. 1534 -1544, 2018.
[15] Y. Bekakra and D. Ben Attous, "Sliding mode controls of active and reactive power of a DFIG with MPPT for variable speed wind energy conversion," *Australian journal of basic and applied sciences*, vol. 5, no. 12, pp. 2274-2286, 2011.
[16] Z. L. Jerbi, *et al.*, "A fuzzy logic supervisor for active and reactive power control of a variable speed wind energy conversion system associated to a flywheel storage system," *Electric power systems research*, vol. 79, pp. 919-925, 2009.
[17] A. Aissaoui, *et al.*, "A Fuzzy Logic Control for Synchronous Machine," *Journal of Electrical Engineering Elektrotechnicky Casopis (JEEEC)*, vol. 58, no. 5, pp. 285–290, 2007.
[18] A. Aissaoui, *et al.*, "Fuzzy logic theory and sliding mode for a self-controlled sychronous machine," *Rev. Roum. Sci. Techn. – Electrotechn Energ*,vol. 52,no. 1, pp. 89-104, 2007.
[19] M. Ali Dami, *et al.*, "Doubly Fed Induction Generator, With Crow-Bar System, under Micro-Interruptions Fault" *International Journal on Electrical Engineering and Informatics*, vol. 2, no. 3, pp. 216-231, 2010.
[20] M. Engin, "Sizing and Simulation of PV-Wind Hybrid Power System," *Hindawi Publishing Corporation International Journal of Photoenergy*, vol 2013, 2013, http://dx.doi.org/10.1155/2013/217526.
[21] P. S. Umashankar, *et al.*, "Modeling and Simulation of a PV System using DC-DC Converter," *International Journal of Latest Research in Engineering and Technology (IJLRET),* vol. 1, issue. 2, pp. 09-16, 2015.
[22] A.Talha, "Modeling and Control of a Photovoltaic Generator Equipped with a MPPT Regulator," *4th International Conference on Electrotechnique (ICEL 2009)*, pp. 10-11, Nov. 2009.
[23] S. A. Ardjoun, "Control of a renewable energy system Multisources connected to the electrical network," PhD Thesis in Electrical Engineering, University Djillali Liabes of Sidi-Bel-Abbes, Algeria, 2016.